journal of the mechanical behavior of biomedical materials 112 (2020) 103995

Contents lists available at ScienceDirect

Journal of the Mechanical Behavior of Biomedical Materials

journal homepage: http://www.elsevier.com/locate/jmbbm

# Effect of insertion factors on dental implant insertion torque/energy-experimental results

Baixuan Yang[a,1,*], Ainara Irastorza-Landa[b], Peter Heuberger[b], Heidi-Lynn Ploeg[a,2]

[a] Department of Mechanical Engineering, University of Wisconsin-Madison, 3046 Mechanical Engineering Building, 1513 University Avenue, Madison, WI, 53706, USA
[b] Nobel Biocare Services AG, Balz-Zimmermann-Str.7, 8302, Kloten, Switzerland

ARTICLE INFO

*Keywords:*
Dental implant
Anchorage
Insertion torque
Insertion energy

ABSTRACT

Anchorage of dental implants is quantified with a mechanical engagement to insertion, for example maximum insertion torque (MIT) and insertion energy (IE). Good anchorage of dental implants highly correlates to positive clinical outcomes. However, it is still unclear how bone density, drill protocol, surface finish and cutting flute affect anchorage. In this study, effects of the insertion factors on both MIT and IE were investigated using a full-factorial experiment at two levels: bone surrogate density (0.32 g/cm$^3$ versus 0.48 g/cm$^3$), drill protocol (Ø2.4/2.8 versus Ø2.8/3.2 mm), implant surface finish (machined versus anodized surface) and cutting flute (with versus without). Osteotomies were prepared on rigid polyurethane foam blocks with dimensions of 40 × 40 × 8 mm. Screw shaped dental implants with variable tapered body were consecutively inserted into and removed from the polyurethane foam blocks three times under constant axial displacement and rotational speed. Axial force and torque were recorded synchronously. Insertion energy was calculated from the area under the torque-displacement curve. In this study, we found the main insertion mechanics were thread forming for the first insertion. For the second and third insertions, the main mechanics shifted to thread tightening. Maximum insertion torque (MIT) responded differently to the four insertion factors in comparison to IE. Bone surrogate density, drill protocol and surface finish had the largest main effects for first MIT. For the first IE, drill protocol, surface finish and cutting flute were significant contributors. These results suggest that MIT and IE are influenced by different mechanics: the first MIT and the first IE were sensitive to thread tighten and forming, respectively. Together MIT and IE provide a complete assessment of dental implant anchorage.

## 1. Introduction

Rehabilitation of missing teeth with dental implants has become a standard procedure over the last 50 years, and the success rate of dental implants has been demonstrated to be related to osseointegration (Caouette et al., 2013), “a direct structural and functional connection between ordered, living bone, and the surface of a load carrying implant”(Branemark et al., 2001). Micromotion between the bone and the implant above 50–150 μm ( Szmukler-Moncler et al., 1998) can cause fibrous tissue formation, resulting in a delay or absence of osseointegration (Javed and Romanos, 2010). Anchorage is quantified as the mechanical engagement of the dental implant during insertion. In the clinic, the anchorage is quantified by maximum insertion torque (MIT) during implant placement, which has been shown to correlate with stiffness of the bone-implant system (O’Sullivan et al., 2000; Quesada-Garcia et al., 2009; Rabel et al., 2007; Swami et al., 2016). Therefore, anchorage of dental implants plays an important role to achieve osseointegration in immediate loading protocols (Mathieu et al., 2014). Several factors, including bone density, surgical drill protocol, and implant design features, affect implant anchorage. However, it is not well understood how these factors and their interactions promote anchorage.

Given a specific implant design, surgeons select a drill protocol based on the bone density and quality. For low bone density and quality, a small, even under-sized drill protocol is a common clinical strategy to enhance anchorage (O’Sullivan et al., 2000; Alghamdi et al., 2011;

* Corresponding author.
*E-mail addresses:* 18by8@queensu.ca (B. Yang), ainara.irastorzalanda@nobelbiocare.com (A. Irastorza-Landa), peter.heuberger@nobelbiocare.com (P. Heuberger), heidi.ploeg@queensu.ca (H.-L. Ploeg).
[1] Present address: Kingston General Hospital, Human Mobility Research Centre, 76 Stuart Street, Kingston, ON, Canada, K7L 2V7.
[2] Present address: McLaughlin Hall, room 303B, 130 Stuart Street, Kingston, ON, K7L 3N6, Canada.

https://doi.org/10.1016/j.jmbbm.2020.103995
Received 21 April 2020; Received in revised form 13 July 2020; Accepted 16 July 2020
Available online 1 August 2020
1751-6161/

Tabassum et al., 2009). In Coelho and co-workers' study, different healing patterns and insertion torque levels were observed for different drill protocols (Coelho et al., 2013). However, high insertion torque does not always guarantee positive clinical outcomes. During the insertion, excessive strain or stress generated by the implant can cause bone resorption (Bashutski et al., 2009).

Implant design features, both macro and micro, such as the cutting flute and surface finish also affect clinical outcomes. Self-tapping implants were designed for bones with poor quality (Chong et al., 2009). It is reported that a cutting flute can both improve osseointegration and simplify the surgical procedure (Olsson et al., 1995; Martinez et al., 2001). In contrast to the expectation of good anchorage requiring a high insertion torque, a cutting flute can decrease MIT (Jimbo et al., 2014; Bickley and Hanel, 1998; Kim and Lim, 2011; Wu et al., 2012). On the micro scale, a high surface roughness increases MIT and has been shown to benefit osseointegration (Gelb et al., 2013; Huang et al., 2005; Jemat et al., 2015; Rupp et al., 2018; Smeets et al., 2016).

Degidi and co-workers suggested insertion energy (IE), calculated as the integral of torque-angle data, as an assessment measure of anchorage (Degidi et al., 2013). Several other studies have also used insertion energy to quantify the insertion process (Di Stefano et al., 2018, 2019; Park et al., 2012). Although positive correlations have been found between IE, MIT and bone density (Degidi et al., 2013; Di Stefano et al., 2018, 2019), it is still unclear how bone density, drill protocol, cutting flute and surface finish affect MIT and IE. Therefore, the purpose of this study was to investigate how these insertion factors affect maximum insertion torque and insertion energy.

## 2. Materials and methods

A full-factorial experimental design at two levels with four factors ($2^4 = 16$) and three to five repeats was designed to develop a better understanding of the mechanics of dental implant insertion. The four insertion factors were: bone density; drill protocol; implant surface finish; and, cutting flute (Table 1). Commercially available implants, 3.5 mm in maximum diameter, with tapered body, and thread length of 11.5 mm (NobelActive® NP 3.5 × 13 mm, Nobel Biocare AB, Göteborg, Sweden), were modified for this study. Implant geometry with cutting flute is shown in Fig. 1. The two surface conditions were machined and spark anodized titanium oxide, referred to as "machined" and "anodized" from here on.

### 2.1. Bone surrogate preparation

Commercial rigid polyurethane (PU) foams (SKU 1522-03, 20 PCF, and SKU 1522-04,30 PCF, Sawbones, Pacific Research Laboratories Inc, WA, USA) were used as bone surrogates with two densities (low: 0.32 g/cm$^3$ and high: 0.48 g/cm$^3$) (Tabassum et al., 2009; Chong et al., 2009). With reference to ASTM standard D1621 (Plastics, 2004), compressive properties of ten surrogate bone blocks of each density were tested on Instron 8521 (Instron, Norwood, MA, USA) and deformation was measured with a dynamic extensometer (Instron 2620-825, 12.5 mm gauge length). The measured mechanical properties are listed in Table 2.

For the implant insertion tests, the bone surrogates were milled to 40 × 40 × 8 mm rectangular blocks. Pilot holes were drilled to 13 mm in depth at the center of bone surrogates (Ø2 mm, Ø2.4/2.8 mm step drill sequence; or Ø2 mm, Ø2.4/2.8 mm, Ø2.8/3.2 mm step drill sequence; Article No. 32297, 32261, 34638, Nobel Biocare AB, Göteborg, Sweden) (Manual and Biocare, 2015). Implant geometry and details of the pilot hole are shown in Fig. 1.

**Table 1**
Four insertion factors with two levels.

| Code | Bone Surrogate Density (g/cm$^3$) | Drill Protocol (mm) | Surface Finish | Cutting Flute |
|---|---|---|---|---|
| 1 | 0.48 | 2.8/3.2 | Anodized | Yes |
| 0 | 0.32 | 2.4/2.8 | Machined | No |

### 2.2. Insertion tests

Insertion tests were performed on an Electroforce 3230-AT Series III (TA instruments, ElectroForce Systems Group, Eden Prairie, Minnesota, USA). Implants were inserted into bone surrogates to 11.5 mm depth (Fig. 1). Collar of the implants was left above the bone surrogate. The implant was rotated clockwise with respect to the bone block, with a speed of 7.5 rpm to 1725° while the bone block was moved vertically with an axial speed of 0.3 mm/s (based on the implant pitch). Once the block reached 11.5 mm, the implant was rotated counter-clockwise with respect to the bone block with a speed of 7.5 rpm to −1725°, while the bone block was moved upward to the original position with a speed of 0.3 mm/s. Each implant was inserted and removed three times consecutively for each test. A new implant was used for each test, and implants were not cleaned between the three insertion/removal cycles (in total, 64 implants were used). Simultaneous axial force, torque, angle and displacement data were recorded at a data acquisition rate of 1024 points per second. Fig. 2 shows the experimental setup. All tests were performed at room temperature in dry conditions. Insertion energy was calculated from initial insertion until 30.1 rad (1725°, corresponding to 11.5 mm and double thread pitch of 2.4 mm) as the areas under insertion torque-twist angle curves.

To protect the load cell from overloading, implants with anodized surface were manually placed in the PU foam blocks with high density and 2.4/2.8 mm drill protocol using a digital torque wrench (DID-4A, Electromatic Equipment Co., Inc., Cedarhurst, NY, USA). These tests were simple insertions and not three insertions-removal cycles, as described above. Insertion rate was not controlled. As displacement data were not recorded, insertion energy could not be calculated for these tests. Therefore, only the first maximum insertion torques were obtained in the manual insertion tests for the two cases.

### 2.3. Statistics

Statistical analyses were performed using IBM SPSS Statistics 25 (IBM Corporation, Armonk, New York, USA). Normality of MITs and IEs in each group was checked using the Shapiro-Wilk test with a significance level $\alpha = 0.05$ and it failed to reject the null hypothesis. Effects and interactions of the four insertion factors ($X_i,\ i = 1,2,3,4$) on first maximum insertion torque ($1^{st}$ MIT, $y$) were calculated using a linear full-factorial model. In this model, there were four main effects ($\beta_i, i = 1,2,3,4$), six two-factor interactions ($\beta_{ij}, i,j = 1,2,3,4$ *and* $i \neq j$), four three-factor interactions($\beta_{ijk}, i,j,k = 1,2,3,4$ *and* $i \neq j, j \neq k, k \neq i$), and a four-factor interaction ($\beta_{1234}$):

$$y = \beta_0 + \beta_1X_1 + \beta_2X_2 + \beta_3X_3 + \beta_4X_4 + \beta_{12}X_1X_2 + \beta_{13}X_1X_3 + \beta_{14}X_1X_4 + \beta_{23}X_2X_3 + \beta_{24}X_2X_4 + \beta_{34}X_3X_4 + \beta_{123}X_1X_2X_3 + \beta_{124}X_1X_2X_4 + \beta_{134}X_1X_3X_4 + \beta_{234}X_2X_3X_4 + \beta_{1234}X_1X_2X_3X_4 \quad (1)$$

To examine significant contributors to IE, a hierarchical multiple linear regression analysis (HLR) was performed. Dependent variables ($y$) were each insertion energy. Independent variables were entered in two steps. In step 1, the independent variable was $1^{st}$ MIT without estimated data ( $x_T$). The first HLR model (HLR1) was:

$$y = \alpha_0 + \alpha_Tx_T \quad (2)$$

In step 2 (the second HLR model, HLR2): the four design factors (bone surrogate density ($x_B$), drill protocol ($x_D$), surface finish ($x_S$) and cutting flute ($x_C$) were added into HLR 1 model:

$$y = \alpha_0 + \alpha_Tx_T + \alpha_Bx_B + \alpha_Dx_D + \alpha_Sx_S + \alpha_Cx_C \quad (3)$$

In the hierarchical regression, three null hypotheses were tested in the following order: (1) the $1^{st}$ MIT was not a significant predictor of IE;

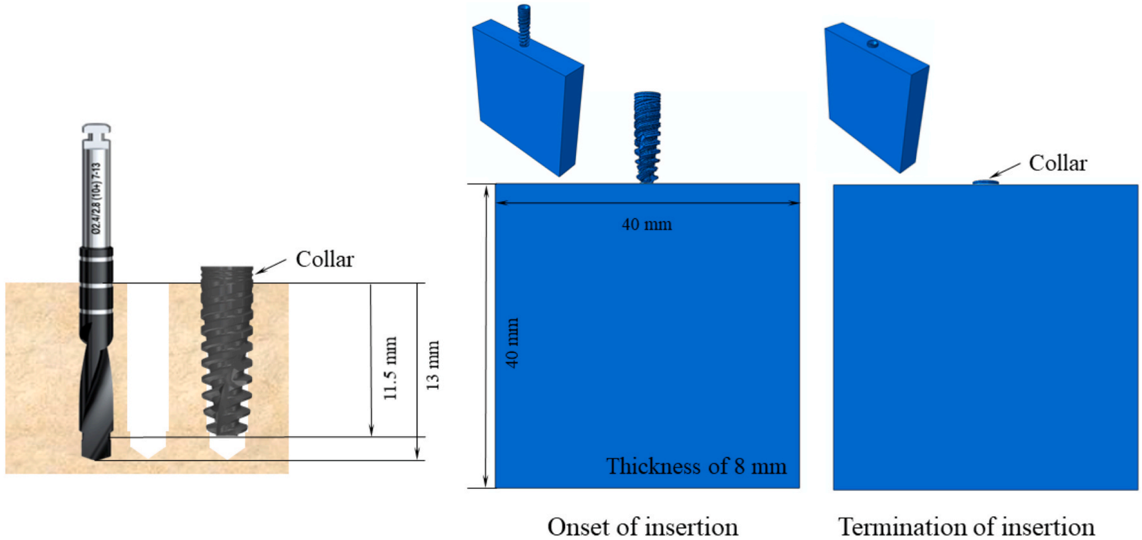


**Fig. 1.** Drill and insertion depth. Pilot holes were stepped with either Ø2.4/2.8 mm or Ø2.8/3.2 mm.

**Table 2**
Compressive properties of bone surrogates: mean (standard deviation).

| Model | Density (g/cm$^3$) | Compressive strength (MPa) | Compressive modulus (MPa) |
|---|---|---|---|
| 20 PCF | 0.32 (8.73 × $10^{-4}$) | 8.16 (0.10) | 304 (15.4) |
| 30 PCF | 0.48 (3.15 × $10^{-3}$) | 17.7 (0.05) | 614 (29.4) |

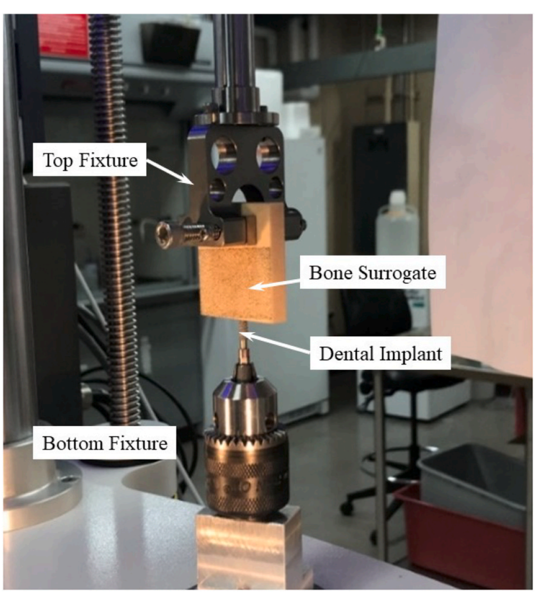


**Fig. 2.** Dental Implant insertion test setup.

(2) the four insertion factors and 1$^{st}$ MIT as a set cannot significantly predict IE; and, (3) none of the four insertion factors account for a significant amount of unique variance. Normality tests were performed on the residuals of HLR using the Shapiro-Wilk test with a significance level $\alpha = 0.05$.

First maximum insertion torque with and without manual data, second maximum insertion torque (2$^{nd}$ MIT) and third maximum insertion torque (3$^{rd}$ MIT) were compared to each other by student two-tailed t-tests; and, the same analyses were performed on first insertion energy (1$^{st}$ IE), second insertion energy (2$^{nd}$ IE) and third insertion energy (3$^{rd}$ IE). Statistical significance is indicated with an asterisk for $p \leq 0.05$.

## 3. Results and discussion

### 3.1. Insertion torque and insertion energy results

Sixty-four (64 = (2$^4$–1) × 3–5 repeats) insertion tests performed on an Electroforce 3230-AT Series III (Fig. 3). To protect the load cell from overloading, tests were not completed on the materials testing machine for the cases: anodized surface, high density and small Ø2.4/2.8 mm drill protocol, for both with and without cutting flute. Manual insertion data for these two cases were used to estimate the missing 1$^{st}$ MIT data. However, 2$^{nd}$ MIT, 3$^{rd}$ MIT and IE for the two cases were not recorded.

Both MIT and IE dropped after first insertion. Pooled 1$^{st}$ MIT without estimated data was 12.5% higher than the 2$^{nd}$ MIT while the 2$^{nd}$ MIT was 5% higher than 3$^{rd}$ MIT with $p < 0.001$ (Fig. 4 and Table s1). IE dropped 69.9% on average from 1$^{st}$ IE to 2$^{nd}$ IE and 15.6% from 2$^{nd}$ IE to 3$^{rd}$ IE with $p < 0.001$ (Fig. 4 and Table s1). In the two estimated groups, cracks were observed in six samples during insertions at the end of insertion, shown in Fig. 3 (c). MIT was recorded when cracks occurred. Comparison tests on other combinations found the MIT was roughly 12.8% less when manually inserted in comparison to the testing machine results with $p < 0.001$.

### 3.2. Full factorial analysis results

In order to assess the effects of each factor on 1$^{st}$ MIT, a linear full factorial analysis (Eq. (1)) was performed. All main factors significantly affected 1$^{st}$ MIT to different degrees (Fig. 5 and Table s2): high bone density, small drill protocol, anodized surface and implant without cutting flute increased 1$^{st}$ MIT by 20 Ncm, 12 Ncm, 9.4 Ncm, and 3.8 Ncm, respectively (Fig. 6). Most interactions were significant. In addition, the effects of some interactions exceeded the main effect of the cutting flute. For instance, the interactions between the bone surrogate density and drill protocol were greater than those for the cutting flute (Fig. 6 and Table s2). Effects for the 2$^{nd}$ and 3$^{rd}$ MIT were not computed in this study due to the missing data. However, correlations of determination ($R^2$) between 1$^{st}$ MIT and 2$^{nd}$ MIT or 3$^{rd}$ MIT were high (0.98 and 0.97, respectively).

Insertion energy was predicted using two HLR models (Eqs (2) and (3)). Residuals for 1$^{st}$ IE and 2$^{nd}$ IE had normal distributions ($p = 0.30$

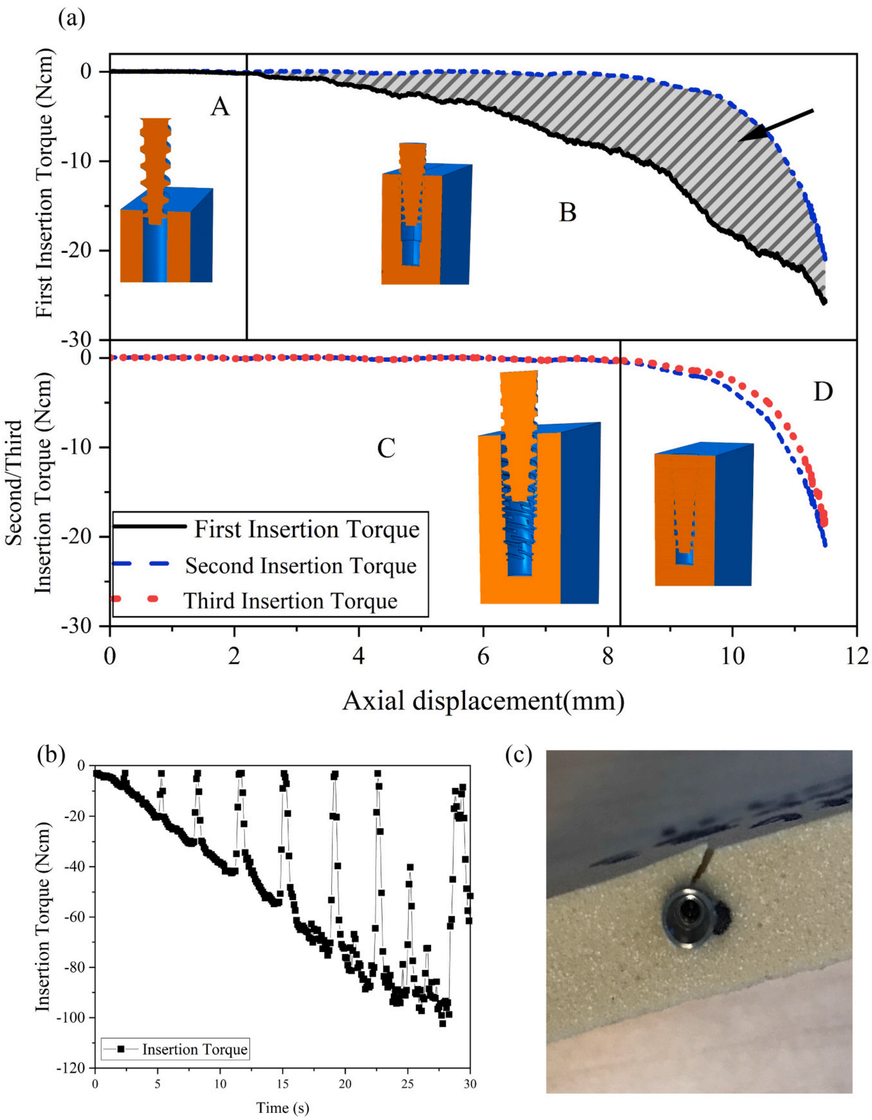


**Fig. 3.** (a) Insertion torques for Ø2.4/2.8 mm drill protocol, low density bone and implants with cutting flute and anodized surface from an insertion test performed on the machine; the arrow shows energy difference between first and second insertion torque. A: entrance phase for the first insertion; B: forming/tightening phase for the first insertion; C: entrance phase for the second and third insertions; D: tightening phase for the second and third insertions. (b) insertion torque for Ø2.4/2.8 mm drill protocol, high density bone, implants without cutting flute and anodized surface for manual insertion; and, (c) crack in bone surrogate after insertion.

and 0.12, respectively). Since the residual for the 3rd IE did not follow a normal distribution ($p < 0.001$) there is no further discussion on 3rd IE. From the HLR1, 1st MIT significantly predicted 1st IE or 2nd IE ($F(1,62) = 1.0 \times 10^3$, $p < 0.0010$ and $F(1,62) = 4.8 \times 10^2$, $p < 0.0010$; $R^2$ were 0.94 and 0.89, for the first and second insertion, respectively). From the HLR2, 1st MIT and four design factors as a set could predict 1st IE or 2nd IE ($F(5,58) = 4.9 \times 10^2$, $p < 0.0010$ and $F(5,58) = 2.1 \times 10^2$, $p < 0.0010$; $R^2$ were 0.98 and 0.95, for the first and second insertion, respectively). The third hypothesis tested if any design factor would contribute to the IE besides 1st MIT. The results showed that drill protocol, surface finish, and cutting flute accounted for significant amounts of variance in 1st IE (Table 3). For the 2nd IE, drill protocol became insignificant. In addition, effects of the surface finish increased 64% for the second insertion (standardized coefficient was 0.11 and 0.18 for 1st IE and 2nd IE, respectively). Another interesting result was that bone density did not contribute to IE even though it had the greatest effect on 1st MIT.

## 4. Discussion

The anchorage of a dental implant depends on mechanical engagement with the bone during the insertion and is reflected by MIT and IE (Degidi et al., 2013; Di Stefano et al., 2018, 2019; Park et al., 2012). This study in the bone surrogate showed that 1st MIT and IE responded differently to various insertion mechanics. Bone density, drill protocol, surface finish, and cutting flute influenced the 1st MIT and IE to different degrees. Therefore, 1st MIT and IE together can provide a comprehensive measurement of anchorage.

During implant insertion resistive torque is created from thread cutting and tightening. After first insertion, the insertion mechanics were dominated by tightening of the implant's thread as opposed to forming threads. During the tightening phase, the insertion torque should overcome the resistive torques due to friction at tapered interface and on the thread inclined plane. The insertion torque curve reflected this shift. Two phases were defined on the insertion torque curves. For the first insertion torque (1st IT), the two phases are entrance and forming/tightening, labeled by A and B in Fig. 3. During the entrance phase, torque did not increase due to a gap between the implant and pilot hole in the bone surrogate. In the second phase, threads were formed, and the pilot hole was enlarged. Entrance and tightening phases were the two phases for second insertion torque (2nd IT) and third insertion torque (3rd IT) (labeled by C and D, respectively, in Fig. 3). Due to the tapped and enlarged pilot hole, the entrance phases were longer than the one of 1st IT. The tighten phases started close to the final turn of placement and the torque rose sharply for this last rotation.

Maximum insertion torque and IE were sensitive to different

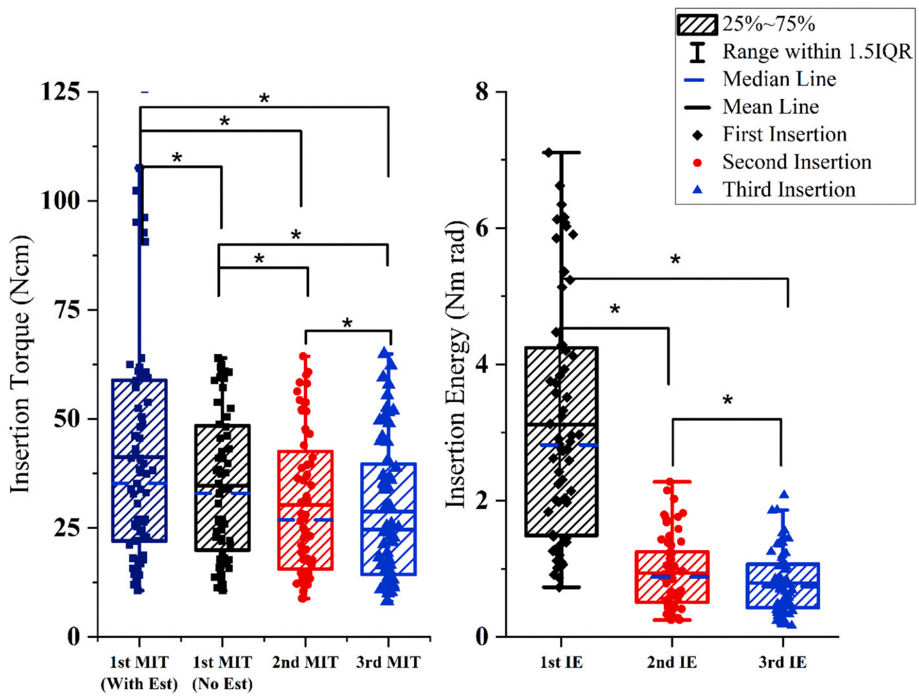


**Fig. 4.** Box-and-whisker plots of maximum insertion torque and insertion energy for all samples. 1st MIT (With Man) included and 1st MIT (No Man) did not include the estimated data. Statistical significance is indicated with * for $p \leq 0.05$.

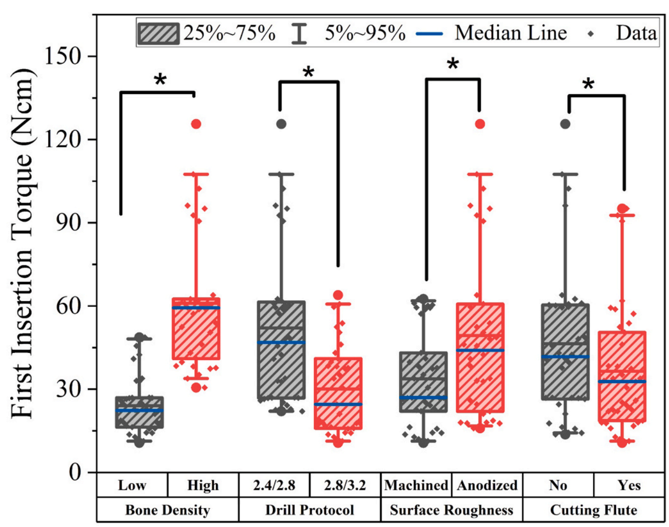


**Fig. 5.** Main effects showing first maximum insertion torque with manual data from the low and high level for each factor.

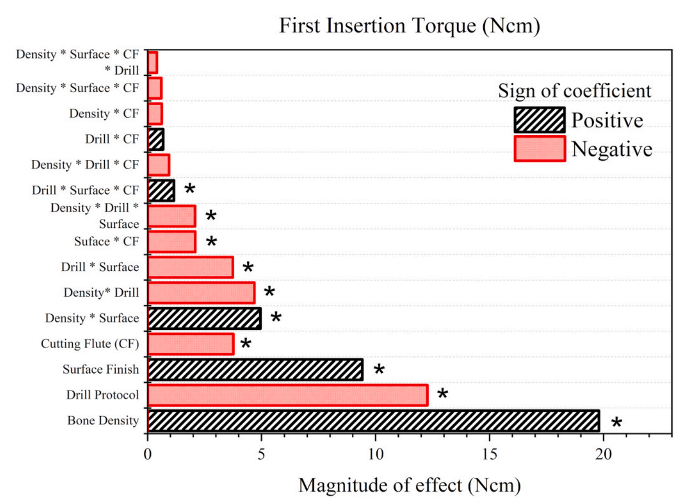


**Fig. 6.** Magnitude of effects on first maximum insertion torque with manual data including main effects and interactions. Statistical significance is indicated with * for $p \leq 0.05$.

insertion mechanics. Maximum insertion torque reflects more on thread tightening than forming, which dropped 12.5% on average between first and second insertions. It also dropped slightly between the second and third insertions, which may be associated with implant settling. For example, rough regions may have become smoother after each insertion; the contact area between the implant and bone surrogate may have decreased; and therefore, MIT dropped slightly.

On the other hand, $1^{st}$ IE is sensitive to the forming process. During the insertion, IE was mainly dissipated into three categories: bone surrogate damage because of thread forming; the thermal energy due to the friction; and strain energy stored in the bone surrogate. However, proportions of each type were different for each repeated insertion. For instance, the forming energy was close to zero after the first insertion. This energy could be estimated by the area between $1^{st}$ IT and $2^{nd}$ IT, shown in Fig. 3 with the arrow. It is important to notice that the percent decrease in IE was 4.6 times larger than that in the MIT from the first to second insertion. This result suggests $1^{st}$ IE is more sensitive to the forming process compared to $1^{st}$ MIT. The reason may be that the MIT is a measurement of the terminal state of implant placement from a single time point; however, the IE depends both on loading history and the MIT (terminal state). The lengths of entrance phases between $1^{st}$ IT and $2^{nd}$ IT or $3^{rd}$ IT were remarkably different. Insertion energy is the integral of torque with respect to rotation. Therefore, $1^{st}$ IE was much different in comparison to $2^{nd}$ IE or $3^{rd}$ IE even with a slight change in MIT.

Since $1^{st}$ MIT and IE were sensitive to different insertion mechanics, the four insertion factors influenced $1^{st}$ MIT and IE to different degrees. An increase in $1^{st}$ MIT may be associated with high bone-implant interface stress or high friction force. In this study, high density bone

**Table 3**
Coefficients of hierarchical multiple linear regression analysis. * for $p \leq 0.05$

| Dependent variable (Nm rad) | Model | Variables | $\alpha$ (Std Error) | Standardized Coefficient | p |
|---|---|---|---|---|---|
| 1st IE | 1 | $\alpha_0$ | −0.38 (0.12) | | *0.0028 |
| | | $\alpha_T$ (1st MIT) | 0.10(0.0032) | 0.97 | *< 0.0010 |
| | 2 | $\alpha_0$ | −0.43 (0.096) | | *< 0.0010 |
| | | $\alpha_T$ (1st MIT) | 0.10 (0.0080) | 0.98 | *< 0.0010 |
| | | $\alpha_B$ (Bone density) | −0.20 (0.26) | −0.056 | 0.46 |
| | | $\alpha_D$ (Drill Protocol) | 0.36 (0.15) | 0.10 | *0.022 |
| | | $\alpha_S$ (Surface Finish) | −0.39 (0.11) | −0.11 | *< 0.0010 |
| | | $\alpha_C$ (Cutting Flute) | 0.20 (0.087) | 0.059 | *0.023 |
| 2nd IE | 1 | $\alpha_0$ | −0.082 (0.052) | | 0.12 |
| | | $\alpha_T$ (1st MIT) | 0.029 (0.0013) | 0.94 | *< 0.0010 |
| | 2 | $\alpha_0$ | 0.017 (0.043) | | 0.70 |
| | | $\alpha_T$ (1st MIT) | 0.024 (0.0036) | 0.77 | *< 0.0010 |
| | | $\alpha_B$( (Bone density) | 0.19 (0.12) | 0.18 | 0.12 |
| | | $\alpha_D$( (Drill Protocol) | 0.089 (0.069) | 0.086 | 0.20 |
| | | $\alpha_S$ (Surface Finish) | −0.18 (0.051) | −0.18 | *< 0.0010 |
| | | $\alpha_C$ (Cutting Flute) | 0.091 (0.039) | 0.088 | *0.025 |

surrogate or small drill protocol, or anodized surface greatly increased 1st MIT (Fig. 6). Maximum stress in a material is limited by its strength. During the first insertion, material was removed in order to form the threads. Stress at the bone-implant interface may be close to the ultimate strength of the bone surrogate. For rigid polyurethane foams, material with higher density has a higher strength (Table 2). Therefore, high bone density increased 1st MIT due to the higher material strength. Another main effect on the interface stress was press-fit between the pilot hole and the implant. Size of pilot holes changes clearances and pressure at the bone-implant interface. Therefore, 1st MIT was greater with the smaller drill protocol by influencing the interface-stress. The third greatest main effect was the surface finish. Different friction coefficients directly affected friction force at the bone-implant interface: the rougher the surface, the higher the 1st MIT. In contrast to these main effects, the cutting flute had a small effect on 1st MIT. The reason may be that the cutting flute was designed to facilitate cutting during the removal, not insertion process. Therefore, the amount of the effect was less than other main effects and even less than some interactions (Fig. 6).

Beside the main effects, the interaction between bone density and drill protocol also had a big effect on the 1st MIT. The drill protocol effect in high density group was significantly higher than in low density group (Fig. 7). High stress level in the bone surrogate can be achieved either by increasing bone density or decreasing the diameter of the drill protocol. For this reason, an under-sized drill protocol for lower density bone is a common clinical strategy to enhance anchorage by increasing 1st MIT (O'Sullivan et al., 2000; Alghamdi et al., 2011; Tabassum et al., 2009). However, a too small diameter of the drill protocol can cause excessive stress in the dense bone surrogate, as demonstrated in the fractured bone surrogate (Fig. 3).

The four insertion factors accounted for significant amount of variance in IE even though the 1st MIT could predict IE on its own. For the 1st IE, drill protocol, surface finish, and cutting flute were significant variables above and beyond 1st MIT. These factors can modify geometric features of either the bone block (drill protocol) or the implant (surface finish and cutting flute). From a mechanics perspective, geometric features govern stress distribution. As a result, these factors contributed to 1st IE by affecting stress distribution during the insertion. For the 2nd IE, the drill protocol became insignificant. Since the threads were already formed, geometric features of the bone block did not change by the initial drill protocol for the second insertion. However, the surface finish and cutting flute were important geometric features of the implant. Therefore, only surface finish and cutting flute influenced 2nd IE as unique contributors. One interesting finding here was that bone density was not a significant contributor to IE even though it had the greatest effect on 1st MIT. This result may further suggest that IE is sensitive to stress distribution instead of the material strength of the bone surrogate. For the same geometric features, the bone surrogates with different densities may be subjected to similarly stress distributions nominalized to their material strength. As a result, the bone density did not significantly contribute to IE.

### 4.1. Limitations

Several study limitations are noted. The laboratory testing environment was different than the clinical situation. Care should therefore be taken when interpreting the results. For the experiment, the implants were inserted under displacement control, which does not mimic the insertion performed by a surgeon with irrigation. This study was performed on rigid polyurethane foams instead of human tissue, and without mimicking the presence of cortical layers. For high density foams, the mechanical strength and modulus are higher than those of the low density foam. It was not clear if high 1st MIT was obtained in the high bone density group because of high bone density and/or higher strength. For human tissue, on the other hand, high bone density does

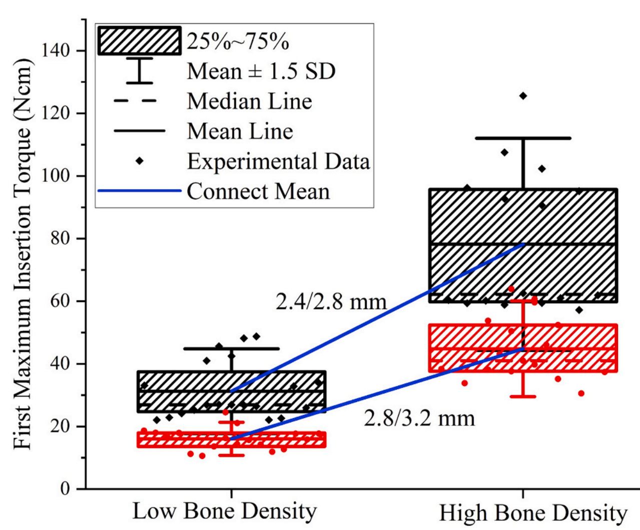


**Fig. 7.** The interaction between bone density and drill protocol was a significant factor for first maximum insertion torque (with manual data).

not guarantee high bone strength (Martin et al., 1998). Future work would be required to investigate the mechanics of implant insertion in human tissue with a force control. In addition, all the results and conclusions were found based on one implant design. Different implant designs may result in results different to those presented here.

A linear full-factorial design of experiment was conducted for this study, but two observations could not be completed. The 1st MIT for these two groups was estimated with manual insertion. From the comparison tests on other groups, the manual insertion torque was 12.8% lower than from the test machine. Therefore, the main effects may have been underestimated. Even though the 1st MIT was estimated by manual placement, the experiment's design was not orthogonal, and two interactions could not be observed. However, with the large total number of runs, $2^4 = 16$, the two missing runs only slightly changed the orthogonality. In addition, the results were found based on statistical analysis. Further studies are required to better understand the clinical implications. However, within the study's limitations, conclusions on implant insertion mechanics are valid.

## 5. Conclusions

Since MIT and IE were sensitive to different mechanics, they responded differently to bone density, drill protocol and implant design features. For the first insertion, the mechanics were dominated by thread forming. For second and third insertions, the main mechanics shifted to thread tightening. Maximum insertion torque, a measurement of the terminal state of implant placement from a single time point, was sensitive to the thread tightening. Bone surrogate density, drill protocol and surface finish significantly affected 1st MIT because these factors directly relate to the stress level or friction force at the bone-implant interface. In contrast, IE depends both on loading history and the MIT (terminal state) and was sensitive to thread forming. Insertion energy was influenced by the stress distribution. The drill protocol, surface finish and cutting flute significantly affected 1st IE. Together, these results suggest that MIT and IE provide distinct measures of anchorage; and therefore, together can provide a more comprehensive assessment of dental implant anchorage.

## CRediT authorship contribution statement

**Baixuan Yang:** Writing - original draft, Investigation, Conceptualization, Methodology. **Ainara Irastorza-Landa:** Conceptualization, Supervision, Writing - review & editing. **Peter Heuberger:** Supervision, Writing - review & editing. **Heidi-Lynn Ploeg:** Conceptualization, Supervision, Writing - review & editing.

## Declaration of competing interest

Ainara Irastorza-Landa and Peter Heuberger are employees of Nobel Biocare Services AG.

## Acknowledgments

We acknowledge funding from Nobel Biocare Services AG (Biomechanics-R 17004/P17047), the support of the Natural Sciences and Engineering Research Council of Canada (NSERC), Ploeg's Research Initiation Grant, and the Human Mobility Research Centre, Queen's University, Kingston, ON, Canada.

## Appendix A. Supplementary data

Supplementary data to this article can be found online at https://doi.org/10.1016/j.jmbbm.2020.103995.

Nomenclature

| | | |
|---|---|---|
| MIT | Maximum insertion torque | Ncm |
| IE | Insertion energy | Nm rad |
| 1st MIT | First maximum insertion torque | Ncm |
| 2nd MIT | Second maximum insertion torque | Ncm |
| 3rd MIT | Third maximum insertion torque | Ncm |
| 1st IE | First insertion energy | Nm rad |
| 2nd IE | Second insertion energy | Nm rad |
| 3rd IE | Third insertion energy | Nm rad |
| Y | Dependent variable | |
| $X_{i,i=1,2,3,4}$ | Independent variables for the linear full-factorial model | |
| $\beta_0$ | Constant for the linear full-factorial model | |
| $\beta_{i,i=1,2,3,4}$ | Main effects for first maximum insertion torque | Ncm |
| $\beta_{ij,i,j=1,2,3,4 \text{ and } i \neq j}$ | Two-factors interactions for first maximum insertion torque | Ncm |
| $\beta_{ijk,i,j,k=1,2,3,4 \text{ and } i \neq j, j \neq k, k \neq i}$ | Three-factors interactions for first maximum insertion torque | Ncm |
| $\beta_{1234}$ | Four-factors interactions for first maximum insertion torque | Ncm |
| HLR | Hierarchical multiple linear regression analysis | |
| HLR1 | First hierarchical multiple linear regression model | |
| HLR2 | Second hierarchical multiple linear regression model | |
| $x_T$ | Independent variable (first maximum insertion torque) | |
| $x_B$ | Independent variable (bone surrogate density) | |
| $x_D$ | Independent variable (drill protocol) | |
| $x_S$ | Independent variable (surface finish) | |
| $x_C$ | Independent variable (cutting flute) | |
| $\alpha_0$ | Constant for the hierarchical multiple linear regression model | |
| $\alpha_T$ | Coefficient for first maximum insertion torque | $10^2$ rad |
| $\alpha_B$ | Coefficient for bone density | Nm rad |
| $\alpha_D$ | Coefficient for drill protocol | Nm rad |
| $\alpha_S$ | Coefficient for surface finish | Nm rad |
| $\alpha_C$ | Coefficient for cutting flute | Nm rad |
| 1st IT | First insertion torque | Ncm |
| 2nd IT | Second insertion torque | Ncm |
| 3rd IT | Third insertion torque | Ncm |

## References

Alghamdi, H., Anand, P.S., Anil, S., 2011. Undersized implant site preparation to enhance primary implant stability in poor bone density: a prospective clinical study. J. Oral Maxillofac. Surg. 69 (12), e506–e512.

Bashutski, J.D., D'Silva, N.J., Wang, H.L., 2009. Implant compression necrosis: current understanding and case report. J. Periodontol. 80 (4), 700–704.

Bickley, M.B.T., Hanel, D.P., 1998. Self-tapping versus standard tapped titanium screw fixation in the upper extremity. J. Hand Surg. 23 (2), 308–311.

Branemark, R., et al., 2001. Osseointegration in Skeletal Reconstruction and Rehabilitation: a Review, vol. 38, pp. 175–182, 2.

Caouette, C., et al., 2013. A New Interface Element with Progressive Damage and Osseointegration for Modeling of Interfaces in Hip Resurfacing, vol. 227, pp. 209–220, 3.

Chong, L., et al., 2009. Effect of implant design on initial stability of tapered implants. J. Oral Implantol. 35 (3), 130–135.

Coelho, P.G., et al., 2013. Biomechanical evaluation of undersized drilling on implant biomechanical stability at early implantation times. J. Oral Maxillofac. Surg. 71 (2), e69–75.

Degidi, M., et al., 2013. Development of a new implant primary stability parameter: insertion torque revisited. Clin. Implant Dent. Relat. Res. 15 (5), 637–644.

Di Stefano, D.A., et al., 2018. The insertion torque-depth curve integral as a measure of implant primary stability: an in vitro study on polyurethane foam blocks. J. Prosthet. Dent 120 (5), 706–714.

Di Stefano, D.A., et al., 2019. Correlation between implant geometry, bone density, and the insertion torque/depth integral: a study on bovine ribs. Dent. J. 7 (1).

Gelb, D., et al., 2013. Clinical and radiographic evaluation of branemark implants with an anodized surface following seven-to-eight years of functional loading. Int J Dent 2013, 583567.

Huang, Y.H., et al., 2005. Bone formation at titanium porous oxide (TiUnite) oral implants in type IV bone. Clin. Oral Implants Res. 16 (1), 105–111.

Javed, F., Romanos, G.E., 2010. The role of primary stability for successful immediate loading of dental implants. A literature review. J. Dent. 38 (8), 612–620.

Jemat, A., et al., 2015. Surface modifications and their effects on titanium dental implants. BioMed Res. Int. 2015, 791725.

Jimbo, R., et al., 2014. The impact of a modified cutting flute implant design on osseointegration. Int. J. Oral Maxillofac. Surg. 43 (7), 883–888.

Kim, Y.S., Lim, Y.J., 2011. Primary stability and self-tapping blades: biomechanical assessment of dental implants in medium-density bone. Clin. Oral Implants Res. 22 (10), 1179–1184.

Manual, NobelActive, Biocare, N. (Eds.), 2015. Nobel Biocare.

Martin, R.B., et al., 1998. Skeletal Tissue Mechanics, vol. 190. Springer.

Martinez, H., et al., 2001. Optimal Implant Stabilization in Low Density Bone, vol. 12, pp. 423–432, 5.

Mathieu, V., et al., 2014. Biomechanical determinants of the stability of dental implants: influence of the bone-implant interface properties. J. Biomech. 47 (1), 3–13.

O'Sullivan, D., et al., 2000. Measurements Comparing the Initial Stability of Five Designs of Dental Implants: a Human Cadaver Study, vol. 2, pp. 85–92, 2.

Olsson, M., et al., 1995. MkII-A Modified Self-Tapping Brånemark Implant: 3-Year Results of a Controlled Prospective Pilot Study, vol. 10, 1.

Park, K.J., et al., 2012. The Relationship between Implant Stability Quotient Values and Implant Insertion Variables: a Clinical Study, vol. 39, pp. 151–159, 2.

Plastics, A.C.D.-o., 2004. Standard Test Method for Compressive Properties of Rigid Cellular Plastics. ASTM International.

Quesada-Garcia, M.P., et al., 2009. Measurement of dental implant stability by resonance frequency analysis: a review of the literature. Med. Oral Patol. Oral Cir. Bucal 14 (10), e538–e546.

Rabel, A., Kohler, S.G., Schmidt-Westhausen, A.M., 2007. Clinical study on the primary stability of two dental implant systems with resonance frequency analysis. Clin. Oral Invest. 11 (3), 257–265.

Rupp, F., et al., 2018. Surface characteristics of dental implants: a review. Dent. Mater. 34 (1), 40–57.

Smeets, R., et al., 2016. Impact of dental implant surface modifications on osseointegration. BioMed Res. Int. 2016, 6285620.

Swami, V., Vijayaraghavan, V., Swami, V., 2016. Current trends to measure implant stability. J. Indian Prosthodont. Soc. 16 (2), 124–130.

Szmukler Moncler, S., et al., 1998. Timing of Loading and Effect of Micromotion on Bone–Dental Implant Interface: Review of Experimental Literature, vol. 43, pp. 192–203, 2.

Tabassum, A., et al., 2009. Influence of the surgical technique and surface roughness on the primary stability of an implant in artificial bone with a density equivalent to maxillary bone: a laboratory study. Clin. Oral Implants Res. 20 (4), 327–332.

Wu, S.W., et al., 2012. The effects of flute shape and thread profile on the insertion torque and primary stability of dental implants. Med. Eng. Phys. 34 (7), 797–805.